Polish Journal of Veterinary Sciences Vol. 22, No. 3 (2019), 589–598

DOI 10.24425/pjvs.2019.129968

Original article

Porcine insulin receptor substrate 2: molecular cloning, tissues distribution, and functions in hepatocyte and aortic endothelial cells

Z. Yin[1,2,*], M. Cai[2,*], X. Weng[2], Z. Liu[2], G. Zhang[1]

[1] College of Animal Science and Technology, Northeast Agricultural University, Harbin 150030, China
[2] Key Laboratory of Animal Cellular and Genetics Engineering of Heilongjiang Province, College of Life Science, Northeast Agricultural University, Harbin 150030, China

Abstract

Insulin receptor substrate 2 (IRS-2) modulates the phosphatidylinositol 3-kinase (PI3K)/Akt pathway, which controls the suppression of gluconeogenic genes; IRS-2 is also a critical node of insulin signaling. Because of the high homology between pig and human *IRS-2*, we investigated the expression pattern and function of porcine IRS-2. QPCR and immunoblotting were used to detect the IRS-2 expression level in different tissues. There were high IRS-2 levels in the cerebral cortex, hypothalamus, and cerebellum in the central nervous system. In peripheral tissues, IRS-2 was expressed at relatively high levels in the liver. Immunohistochemistry analysis revealed that IRS-2 was mainly distributed in the hypothalamus and cerebral cortex. Furthermore, *IRS-2* knockdown porcine hepatocytes and porcine aortic endothelial cells (PAECs) were generated. The *IRS-2* knockdown induced abnormal expression of genes involved in glycolipid metabolism in hepatocytes and reduced the antiatherosclerosis ability in PAECs. In addition, we disrupted IRS-2 in porcine embryonic fibroblasts (PEFs) using the CRISPR/Cas9 genome editing system, before finally generating IRS-2 knockout embryos by somatic cell nuclear transfer (SCNT). Taken together, our results indicate that *IRS-2* might be a valuable target to establish diabetes and vascular disease models in the pig.

Key words: IRS-2, molecular cloning, hepatocytes, aortic endothelial cells

Introduction

Insulin receptor substrate (IRS), a key mediator of insulin and insulin-like growth factor (IGF)-I signaling, modulates cell growth, differentiation, glucose metabolism, and gene expression. IRS-1 and IRS-2 are key members of the insulin receptor substrate family. Disruption of IRS-1 in mice retards growth, but diabetes does not develop because insulin secretion increases to compensate for the mild resistance to insulin (Araki et al. 1994), whereas *IRS-2*-deficient mice show progressive deterioration of glucose homeostasis because of insulin resistance and a lack of beta-cell compensation for this insulin resistance (Withers et al. 1998, Kubota et al. 2000). In addition, it has been shown that IRS-2 can integrate the effects of insulin in peripheral

Correspondence to: G. Zhang, e-mail: Gxzhang@neau.edu.cn
* These authors contributed equally to this work.

tissues with IGF-1 in beta-cells to maintain glucose homeostasis (Withers et al. 1999). Therefore, in mice, IRS-2 dysfunction may contribute to the pathophysiology of type 2 diabetes. In humans, a number of polymorphisms have been identified in the *IRS-2* gene. *IRS-2* polymorphisms have been associated with decreased insulin sensitivity and impaired glucose tolerance in some populations (El Mkadem et al. 2001, Stefan et al. 2003).

Pigs are an important model species for biomedicine. Pigs have similar physiology (such as cardiovascular anatomy and function, metabolism, lipoprotein profile, size, tendency to become obese, and omnivorous habits) to humans (Fan and Lai 2013, Zhang and Lerman 2016). In addition, the longevity of pigs makes it possible to investigate the pathogenesis of disease and to assess the efficacy and side effects of treatments. Pigs have been particularly valuable for studying cardiovascular disease and diabetes (Hamamdzic and Wilensky 2013, Wolf et al. 2014, Koopmans and Schuurman 2015). Therefore, elucidation of the function of IRS-2 in pigs would be beneficial for generating swine models of diabetes and cardiovascular disease. However, information about porcine IRS-2 is lacking, and data regarding the expression and function of IRS-2 in porcine tissues and cells are limited.

Here, the full-length cDNA for porcine IRS-2 was cloned, the expression and distribution pattern of IRS-2 in porcine tissues was determined, and its role in regulating cellular glucolipid metabolism and antiatherosclerosis were assessed by generation of *IRS-2* knockdown hepatocytes and porcine aortic endothelial cells (PAECs). Finally, IRS-2 knockout embryos were constructed via CRISPR/Cas9 and somatic cell nuclear transfer (SCNT).

Materials and Methods

Cells, animals, and sampling

Primary hepatocytes were kindly gifted by Dr. Zhou Dong (Northwest A&F University). PAECs were purchased from Applied Biological Materials Inc. (Canada). The porcine embryonic fibroblasts (PEFs) used for SCNT were isolated from a fetal Bama minipig (day 38). The tissue samples were taken from a healthy adult Bama minipig. All animals were treated in strict accordance with the "Guidelines on Ethical Treatment of Experimental Animals" from the Chinese Ministry of Science and Technology. The sampling procedures in this study had received prior approval from the Experimental Animal Manage Committee of Northeast Agricultural University.

Cloning and analysis of porcine IRS-2

Two PCR primers (F1: GAGCGAGAARAAGTG GCGGAGCA; R1: TCTCGGCS-GCYACGGCRAAGTA; F2: GCAACTTTAAAACAAGCGAAA; R2: GACTAAAT-ACAACGCACGACT) for two cDNA fragments of porcine *IRS-2* were designed based on sequence alignments of conserved regions from various species (Human, NM_003749.2; mouse, NM_001081212.1; Rat, NM_001168633.1). Then, the Genome Walking Kit (Takara, Japan) was used to obtain unknown sequences near the conserved regions. After the products were confirmed to be part of the *IRS-2* gene by sequencing, full-length cDNA was obtained based on these fragments using 5'/3'-RACE kit (Roche, Germany).

RNA extraction, cDNA synthesis and QPCR

RNA was isolated from each tissue or cell sample using TRIzol Reagent (Ambion, USA) combined with the RNeasy Kit (Qiagen, Germany) according to the manufacturer's instructions. The final RNA was eluted in an appropriate amount of RNase-free water. The integrity of the RNA extracted from each sample was confirmed by agarose gel electrophoresis, with ethidium bromide staining and visualization under UV light. Complementary DNA was synthesized from the total RNA using M-MLV Reverse Transcriptase (Promega, USA) and was then stored at −80°C until QPCR analysis. Quantitative real-time PCR was performed with the SYBR Premix DimerEraser (Takara Bio, Japan) and an ABI 7500 Real-time PCR System (Applied Biosystems, USA). The sequences of the QPCR primers for *IRS-2* are forward: AGAGCGAGAAGAAGTGGCGGAGCA; reverse: TCCTTGGTGTAG-AGGGCGATCAGGTAC. Each system was reevaluated and optimized for the protocol used, and all reagents were titrated for optimal performance. To quantify the relative mRNA expression, the Ct values of the *IRS-2* genes were normalized to the Ct values of the housekeeping gene encoding *GAPDH* using the $2^{-\Delta\Delta C_T}$ method, and the results were presented as fold changes. The PCR cycling parameters were as follows: initial denaturation at 95°C for 30 s, then 40 cycles at 95°C for 5 s, 55°C for 30 s, and 72°C for 15 s. Each PCR run was followed by a melting-curve stage, and all melting curves displayed a single peak.

Immunoblotting

Tissue or cell lysates were prepared with RIPA buffer (Sigma-Aldrich, USA), according to the manufacturer's instructions. The protein concentrations in the supernatants were determined with the BCA Protein Assay kit (CoWin Biotech, China). Sodium dodecyl

Table 1. Primers of genes related to functions of porcine hepatocytes and PAECs.

Gene	Oligonucleotide primers (5′→3′)	Product length (bp)	GenBank accession number
eNOS	F CCCTACAACGGCTCCCCTC R GCTGTCTGTGTTACTGGATTCCTT	110	AY266137
HO-1	F GGCTGAGAATGCCGAGTT R ATGTAGCGGGTGTAGGCGTGGG	197	NM_001004027.1
VEGFA	F CCCCGATGAGATCGAGTACATCTT R ACCGCCTCGGCTTGTCAC	380	EU714324
VCAM-1	F ACTACCCCTGAGATATGGTG R GTGCCAGTCATATTAAGATGC	235	NM_213891.1
PEPCK	F GGAGATGGCGACTTCGTCAAG R CGAAGGGCAAAGCACTTCTTG	194	NM_001161753.1
FBP-1	F CTCTCCAATGACCTGGTTATTAACG R TTTCTGTAGATGCCAAAGATGGTTC	197	AF073474.1
Gck	F GGCTGGAGACCCACGAAGAG R TGGTGCTTGGTCTTCACACTCC	181	XM_003134883.2
SREBP-1	F TGACCGACATCGAAGACATGC R GGGAGCTGGCATCAGGACTG	126	NM_214157.1
LXRA	F ATCCGCCTGAAGAAACTGAAGC R CTGGTCTGAAAAGGAGCGTCTG	177	AB254405.1
Abcg8	F AGGTCTCACCTACCAGGTGGACATG R TTGTCCGCTCCTCACTCTGAAGC	144	EF472592.1
CYP7a1	F CCGCTTCTGATACCTGTGGACTTAG R CGTCACAACAGAGGCTCCAGC	148	NM_001005352.3
GLUT-1	F TGGGCATGTGCTTCCAGTAT R CTCCTCGGGTGTCTTGTCG	191	KU672521.1
GLUT-2	F CACATCCTGCTTGGTCTATC R CACTTGATGCTTCTTCCCT	202	KU672522.1
GAPDH	F TGTACCACCAACTGCTTGGC R GGCATGGACTGTGGTCATGAG	190	AF017079

sulfate-polyacrylamide gel electrophoresis (SDS-PAGE) 5 × loading buffer (CoWin Biotech) was added to the lysates. The lysates were heated to 100°C for 5 min, after which 30 μg of protein was loaded into each well of a 10% SDS-PAGE gel. The resolved proteins were transferred electrophoretically onto polyvinylidene difluoride membrane (Millipore, USA) and blocked with 5% nonfat milk (BD, USA). The membrane was then incubated with a rabbit anti-IRS-2 monoclonal antibody (diluted 1:2000; Abcam, UK). After incubation overnight at 4°C, the blots were washed and then exposed to the secondary antibody (Peroxidase--Affinipure Goat Anti-rabbit IgG [H+L], diluted 1:20,000; [Sigma]) for 45 min at 37°C; after the membranes were washed, the secondary antibody was then detected with the ECL WB kit (Invitrogen, USA). The beta-tubulin fragment present in each sample was used as the internal control.

Immunohistochemistry

The tissue samples fixed in 4% paraformaldehyde were embedded in paraffin and sectioned into 3 mm, which were collected on silanized slides. Paraffin sections were deparaffinized, rehydrated and boiled in 0.01% citrate buffer for antigen retrieval.Endogenous peroxidase activity was quenched with 3% H_2O_2 in methanol for 20 min at room temperature, followed by incubation with goat serum for 30 min. Subsequently, sections were incubated overnight at 4°C in a humidified chamber with a 1:200 dilution of the primary antibody (the same Ab as used in immunoblotting above). IRS-2 was then detected using a commercial immunoperoxidase staining kit (Boster, Nanjing, China). Briefly, the sections were incubated with a 1:200 dilution of biotinylated secondary goat anti-rabbit antibody for 2 h at room temperature, followed by the avidin-biotin-peroxidase complex (ABC) reagent incubation for 1 h. Bound antibody conjugates were visualized using 3,3'-diaminobenzidine (DAB) (Zhongshan Golden Bridge Co., Beijing, China). Negative controls were included in each batch and were performed with the same procedure by replacing the primary antibody with PBS.

Generation and characterization of IRS-2 knockdown hepatocyte and PAEC

For generation of stable IRS-2-knockdown cells, lentivirus vectors expressing short-hairpin RNA (shRNA;

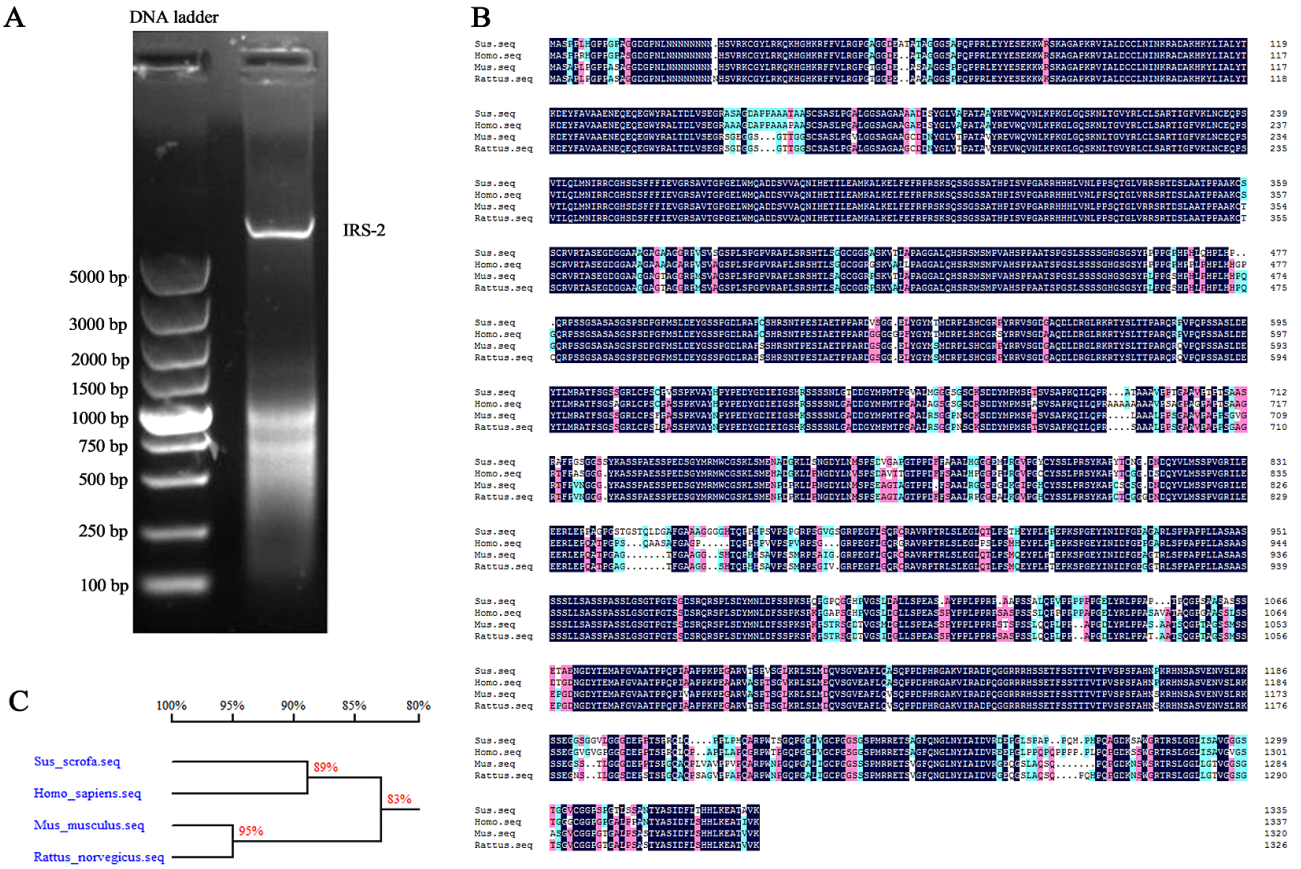

Fig. 1. Gene cloning and bioinformatics analysis of porcine IRS-2.
(A) Full-length cDNA of porcine IRS-2 was obtained. (B) Multiple sequence alignments of porcine IRS-2's deduced amino acid sequence with human, mouse, and rat. (C) Homology comparison of IRS-2 coding sequences among pig, human, mouse, and rat.

sequence: 5'-GGTTTCTGGAGATGGAGATGC-3') targeting pig *IRS-2* and shCtrl sequence (5'- TCCTAAGGTTAAGTCGCCCTCG -3') (constructed by ComateBio company, Changchun, China) were transfected into 293T cells using Lipofectamine LTX (Invitrogen, USA) and lentiviral packaging mix according to the manufacturer's protocol. Hepatocytes and PAECs were then transfected with the lentiviruses at a multiplicity of infection (MOI) of 10 and 100 for hepatocytes and PAECs, respectively. Stable *IRS-2*-knockdown cells were selected with puromycin (Sigma; 0.5 μg/mL for hepatocytes and 0.25 μg/mL for PAECs). The interference efficiency was confirmed by QPCR and Immunoblotting assays. Porcine hepatocyte and PAEC function-related genes expressions were measured by the QPCR method as used above in this study. The primer sequences for these genes are listed in Table 1.

Construction of IRS-2 knockout embryos by CRISPR/Cas9 and SCNT

The CRISPR/Cas9 and SCNT system was used to construct IRS-2 knockout embryos. We initially constructed a lenti-pcas9n-puro-px462 plasmid that contains the Cas9 protein and puromycin-resistance cassette. After a specific guide RNA was inserted into the plasmid, the viruses were packed, and the PEFs were infected. To obtain IRS-2 knockout colonies, cells were selected by puromycin treatment for at least 10 days. The knockout results were verified by PCR and Sanger sequencing, and the gene-disrupted cells were used as nuclear donor cells in the following SCNT procedure. SCNT was performed as described in previous studies (Liu et al. 2008). The cleavage and blastocyst rates were evaluated between wild-type embryos and gene knockout embryos.

Statistical analysis

Statistical significance was analyzed by Student's *t*-test when only two groups were compared or by one-way analysis of variance (ANOVA) when more than two groups were compared. A p value <0.05 was considered statistically significant.

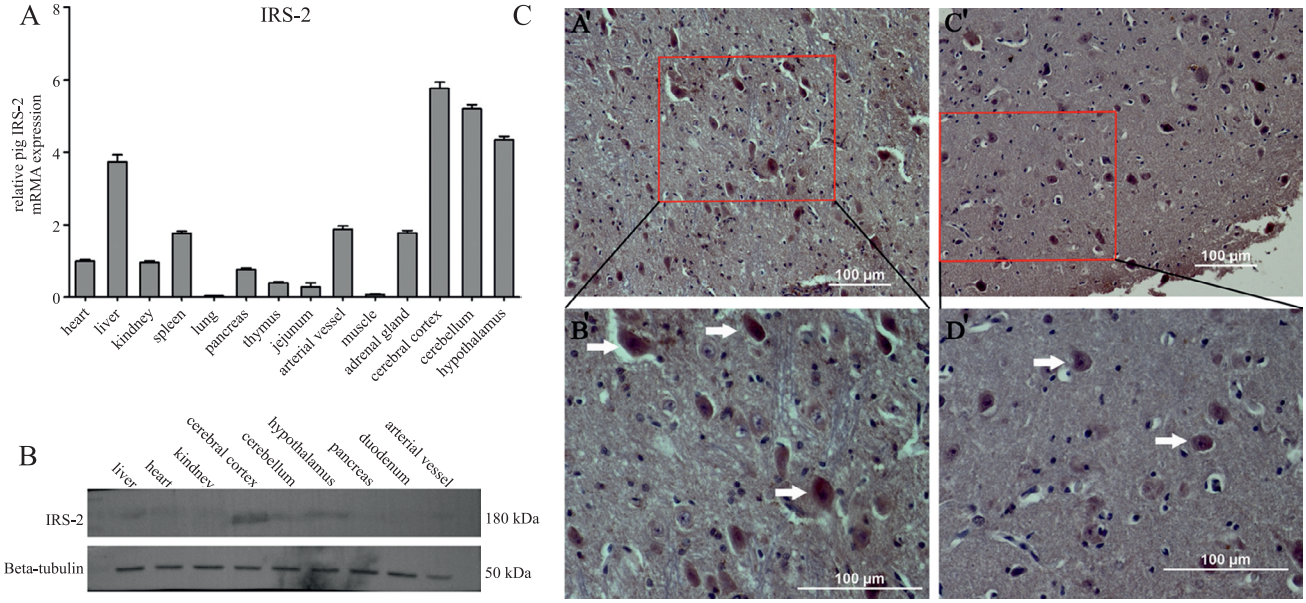

Fig. 2. Porcine IRS-2 expression and distribution in different tissues.
(A) Relative IRS-2 mRNA expression level in different tissues. (B) Relative IRS-2 protein expression level in different tissues. (C) Porcine IRS-2 distribution in hypothalamus and cerebral cortex. A' and B': Representative microphotographs of DAB-stained hypothalamus sections. C' and D': Representative microphotographs of DAB-stained cerebral cortex. The white arrows indicate the cells with high expression level of IRS-2.

Results

Analysis of porcine IRS-2

A gene fragment of porcine IRS-2 (427 bp) was amplified based on sequence homology with mouse, rat and human. Then, 5'/3'-RACE was performed to obtain full-length cDNA. The full cDNA of porcine IRS-2 was 5816 bp, consisting of a 5'-untranslated region (UTR) of 214 bp, a CDS region of 3276 bp, and a 3'-UTR of 2323 bp. The sequence was submitted to GenBank and was assigned an accession number (GenBank ID:MG664849.1). Based on sequence alignment, the nucleotide sequence of the porcine IRS-2 CDS region shared 80.93%, 77.12%, and 78.27% identity with that of human (AH010223.2), mouse (BC147580.1), and rat (NM_001168633.1), respectively (Fig. 1). The deduced amino acid sequence of porcine *IRS-2* was 1092 amino acid residues in length, the estimated molecular weight was 180 kDa, and the theoretical isoelectric point was 8.59. The protein sequence of porcine *IRS-2* shared 89.05%, 84.92% and 83.31% identity to that of human, mouse, and rat, respectively (Fig. 1B).

Expression of IRS-2 in tissues

First, porcine IRS-2 mRNA expression in each tissue was analyzed by QPCR. As shown in Fig. 2A, IRS-2 mRNA was detected in all tested tissues. IRS-2 mRNA levels were high in the cerebral cortex, hypothalamus, and cerebellum. In the peripheral tissues, IRS-2 was expressed at relatively high levels in the liver, whereas its expression levels were comparatively low in jejunum, kidney, heart and pancreas. IRS-2 protein expression in tissues is shown in Fig. 2B. The IRS-2 protein was ~180 kDa, as detected in different pig tissues. The highest expression of IRS-2 protein was observed in the cerebral cortex, cerebellum, and hypothalamus. In contrast, there was almost no expression in the jejunum, kidney, heart and pancreas. Overall, the IRS-2 protein level was correlated with its mRNA expression level.

IRS-2 distribution in hypothalamus and cerebral cortex tissues

Since IRS-2 was highly expressed in the CNS compared to peripheral tissues, we sought to determine the distribution of IRS-2 in the hypothalamus and cerebral cortex. Immunohistochemistry analysis revealed that IRS-2 was localized in the arcuate nucleus, ventromedial nucleus, and parvocellular paraventricular nucleus in the hypothalamus. Moreover, the IRS-2 distribution in those regions appears as scattered staining (Fig. 2C, A', B'). In the cerebral cortex, IRS-2 also showed scattered positive staining (Fig. 2C, C', D').

Generation and characterization of porcine hepatocytes with IRS-2 knockdown

The knockdown effect of IRS-2 was confirmed with QPCR (Fig. 3A and 3B) and immunoblotting (Fig. 3C). The expression of genes related to glucolipid metabo-

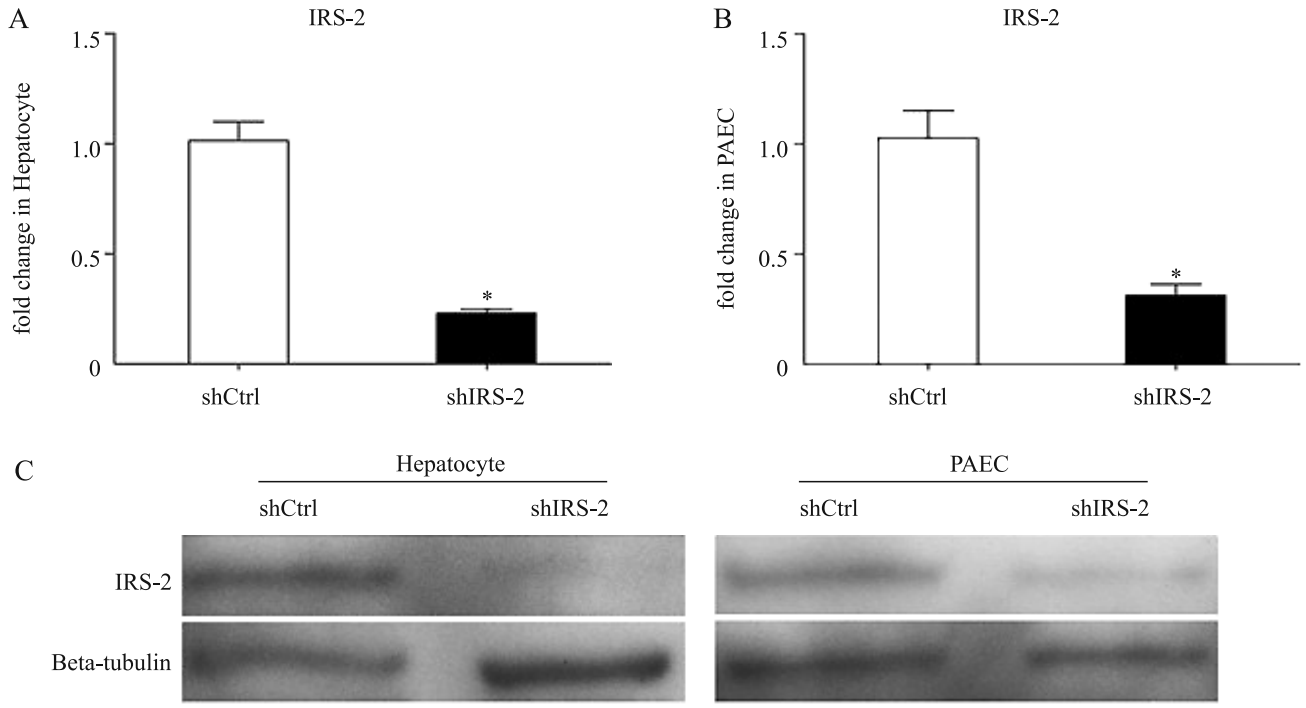

Fig. 3. Generation of hepatocyte and PAEC with IRS-2 knockdown.
(A) QPCR analysis of porcine IRS-2 mRNA level in shCtrl and shIRS-2 groups in hepatocyte. (B) QPCR analysis of porcine IRS-2 mRNA level in shCtrl and shIRS-2 groups in PAEC. (C) The expression level of IRS-2 protein in shCtrl and shIRS-2 groups in hepatocyte and PAEC.

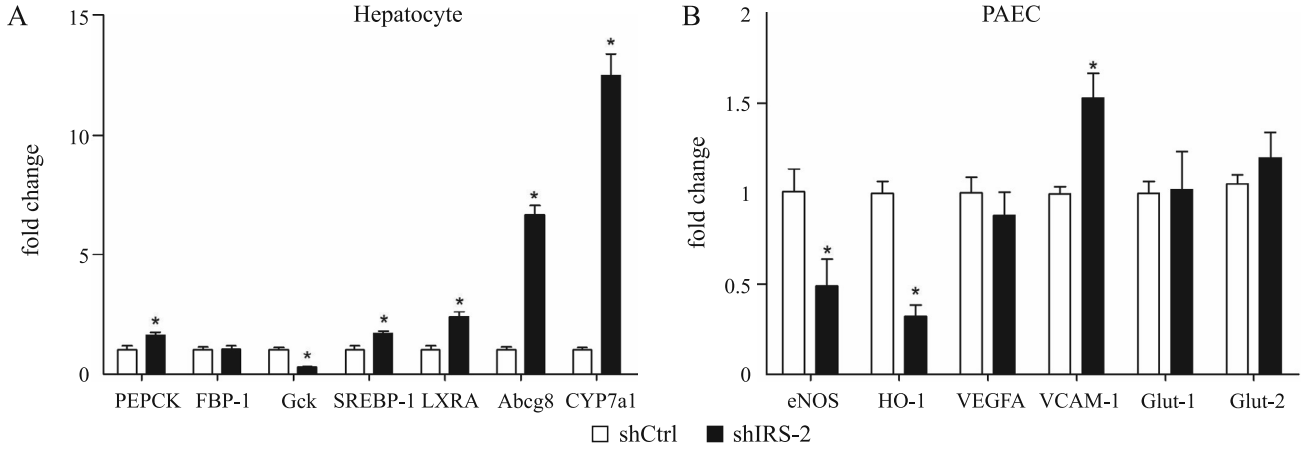

Fig. 4. The effect of IRS-2 knockdown in porcine hepatocyte and PAEC. (A) The expressions of glucose metabolism related genes PEPCK, FBP-1, Gck, and the cholesterol metabolism related genes SREBP-1, LXRA, Abcg8, and CYP7a1 in hepatocyte with IRS-2 knockdown. (B) The mRNA expression of genes including eNOS, HO-1, VEGFA, VACM-1, Glut-1, and Glut-2 were measured by QPCR in PAEC with IRS-2 knockdown.

lism were analyzed. The *PEPCK* mRNA expression level increased remarkably in hepatocytes with *IRS-2* knocked down. The expression of *FBP-1* did not change significantly, whereas the *Gck* mRNA expression show a significant decrease after *IRS-2* knock down. The *SREBP-1* and *LXRA* genes were obviously upregulated in the *IRS-2* KD group. We further detected cholesterol metabolism-related genes that are downstream of LXRA, including *Abcg8* and *CYP7a1*. The results showed that the expression of *Abcg8* and *CYP7a1* significantly increased in *IRS-2* KD cells (Fig. 4A).

Establishment and characterization of PAECs with IRS-2 knockdown

The same method mentioned above was used to establish the *IRS-2* KD PAECs, and the expression of *eNOS, HO-1*, *VEGFA*, *VCAM-1*, *Glut-1*, and *Glut-2* genes was assessed. QPCR results showed that the mRNA expression levels of *eNOS* and *HO-1* were lower obviously in *IRS-2* KD cells. In contrast, the *VCAM-1* mRNA expression was significantly increased in *IRS-2* KD cells. There was no significant change of *VEGFA* mRNA expression after *IRS-2* knock

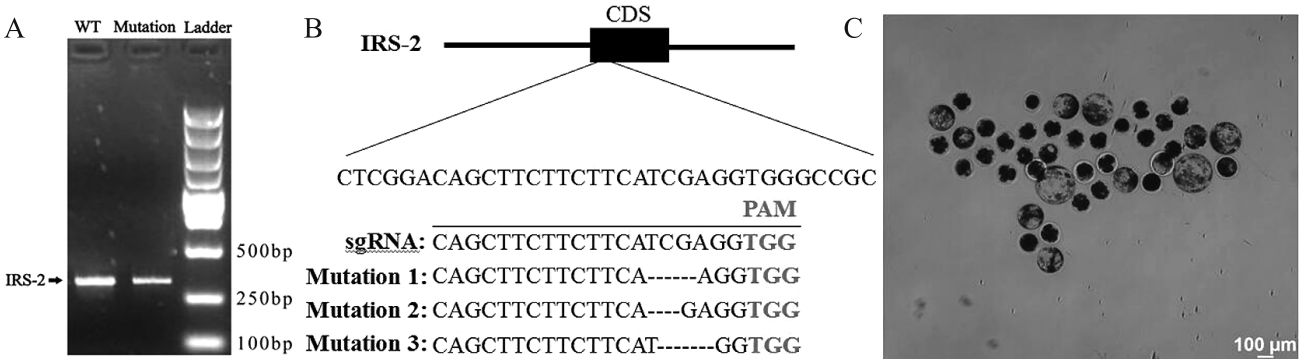

Fig. 5. Construction of *IRS-2* knockout SCNT embryos.
(A) The PCR result of mutation and wild type IRS-2. (B) Sequence muation of *IRS-2* in PEFs based on CRISPR/Cas9 system. (C) The IRS-2 deficient SCNT embryos at blastocyst stage.

Table 2. The cleavage rate and blastocyst rate of *IRS-2* knockout SCNT embryos.

Group	No. of oocytes	Cleavage rate (%)	Blastocyst rate (%)
Control	280	75.62±6.48	20.25±3.23
IRS-2 KO	278	76.33±4.65	19.91±4.03

down. For *Glut-1* and *Glut-2* mRNA expression, the results did not show obvious changes in *IRS-2* KD cells compared to control cells (Fig. 4B).

Construction of IRS-2 knockout SCNT embryos

Three guide RNA candidates (gRNA 1, gRNA 2, and gRNA 3) targeting the porcine IRS-2 gene were synthesized and inserted into lenti-pcas9n-puro-px462 vector. The packed virus containing the porcine IRS-2 gene targeting CRISPR was infected into PEFs, and positive colonies were selected using puromycin. Three colonies were analyzed by Sanger sequencing to identify the exact modifications of IRS-2 at the nucleotide level. Sequencing results are summarized in Fig. 5. The IRS-2-deficient PEFs were used to construct SCNT embryos. The development capacity of IRS-2-deficient embryos was evaluated, and the results showed that the cleavage rate and blastocyst rate were not impacted (Table 2).

Discussion

Here, we cloned the full-length cDNA of porcine *IRS-2* and measured its expression and distribution pattern in different tissues. This work represents the first reported cloning of full-length porcine cDNA of *IRS-2*. Both nucleotide and amino acid sequences of porcine *IRS-2* share higher similarities with human *IRS-2* (80.93% and 89.05%, respectively) than mouse or rat, suggesting that pig and human IRS-2 proteins play similar physiological roles. A recent study reported that the IRS-2 protein has a lower average conservation score than IRS-1 in vertebrate species (Al-Salam and Irwin 2017). Therefore, the relatively high conservation of *IRS-2* nucleotide and amino acid sequences between human and pig indicates that porcine IRS-2 may be a better human disease model target than IRS-2 in mice or rats. QPCR and Immunoblotting results showed that porcine IRS-2 was highly expressed in cerebral cortex, hypothalamus, and cerebellum. This is consistent with results from studies in mouse and rat and indicates that IRS-2 might play important conserved roles in the central nervous system (CNS) in mammals (Choudhury et al. 2005, Pardini et al. 2006). Moreover, we found that the *IRS-2* mRNA has alternative splicing in cerebral cortex tissue (data not shown), suggesting complex functions of IRS-2 in the CNS. In peripheral tissues, IRS-2 is relatively highly expressed in the liver and arteries, suggesting that IRS-2 might play important roles in glucolipid metabolism and vessel function. It has been reported that the expression of IRS-2 in diabetic human liver tissues is reduced to varying degrees (Kerouz et al. 1997). The IHC results showed that IRS-2 is mainly distributed in the arcuate nucleus, ventromedial nucleus, and paraventricular nucleus. The strong staining in those areas indicates the role of IRS-2 in food intake and energy regulation. It has been reported that conditional knockout of IRS-2 in hypothalamic neurons and beta cells could result in insulin resistance with progressive obesity and diabetes (Choudhury et al. 2005). However, unlike the QPCR and immunoblotting data, there is no obvious staining of IRS-2 in the cerebellum (data not shown). In this tissue, the IRS-2 might be expressed in most cells but with a low level in each cell type. In conclusion, the high expression levels of IRS-2 in the cerebral cortex and hypothalamus

tissues indicate its important role in metabolic signaling to the CNS.

The liver is the central organ that regulates the metabolism of nutrients. It can be used to convert postprandial glucose into glycogen, to convert excess glucose into fatty acids and to oxidize fatty acids to sugar (Gribble 2005). The hepatic insulin signaling pathway is important for the regulation of carbohydrate and fat metabolism through the transmission of insulin signals to activate the downstream MAPK/Akt/Foxo1 pathway, which activates glucose transport and regulates fatty acid oxidation. Previously, it has been reported that the hepatic insulin signaling pathway is blocked and causes abnormal glucose and lipid metabolism after double knockdown of *IRS-1* and *IRS-2* genes in mice (Taniguchi et al. 2005). Recently, Kubota et al. found that the development of selective hepatic insulin resistance was characterized by reduced IRS-2 expression and intact IRS-1 expression (Kubota et al. 2016). Therefore, IRS-2 might play a key role in modulating hepatic metabolic homeostasis. In the present study, our results found that knock down of *IRS-2* genes in porcine hepatocytes can lead to a significant upregulation of *PEPCK* gene expression. PEPCK is the first key enzyme in the gluconeogenesis pathway, and the expression level of PEPCK in the liver is related to the blood glucose concentration. For another gluconeogenic enzyme gene, *FBP-1*, we did not find significant expression change in IRS-2 KD cells. We found that the *Gck* gene expression level was significantly reduced after IRS-2 knockout. Gck is the key enzyme in the first step of glycolysis in the liver (Gloyn 2003). If *Gck* gene expression is inhibited, it will affect glycolysis and reduce the glucose content in the plasma. Inappropriate activation of gluconeogenesis is usually accompanied by abnormal lipid metabolism. SREBP-1 is a cholesterol sensor that regulates cholesterol metabolism and plasma cholesterol levels. Increased *SREBP-1* gene expression can lead to an increase in serum cholesterol levels. In the present study, the knockdown of *IRS-2* significantly upregulated the *SREBP-1* gene in hepatocytes. These results implied that IRS-2 might be indispensable for sustaining glucolipid metabolic homeostasis in hepatocytes. Insulin can also regulate lipid metabolism by activating *LXRA*. Therefore, *LXRA* gene expression in *IRS-2* KD cells was measured, and the results showed that *LXRA* expression was remarkably increased after *IRS-2* knockdown. Moreover, we further measured expression of two genes that regulate cholesterol metabolism downstream of the *LXRA*, including *Abcg8* and *CYP7a1,* and we found that the expression levels of these two genes were also increased in *IRS-2* knockdown cells. In summary, these results suggested that IRS-2 induced abnormal glucose metabolism and can also cause abnormal lipid metabolism, further showing that the *IRS-2* gene is critical for the maintenance of normal physiological liver metabolism.

Blood vessels regulate peripheral and systemic glucose homeostasis by transporting glucose to peripheral tissues in response to high systemic glucose levels. Vascular endothelial cells are exposed to elevated glucose and insulin concentrations postprandially in healthy individuals and permanently in patients with metabolic syndrome and diabetes. Moreover, endothelial cells are also routinely exposed to damaging oxidants and cholesterol (Higashi et al. 2009). Therefore, endothelial dysfunction is a key research focus as it is a potential contributor to the pathogenesis of vascular disease in diabetes mellitus. Clarifying the functions of IRS-2 in porcine vascular endothelial cells might provide key information for establishing animal models, as IRS-2 has been considered a key mediator in endothelial insulin signaling (Kubota et al. 2011, King et al. 2016). It has been shown that the activation of eNOS by insulin that produces NO is impaired in insulin resistant states (Huang 2009). As an inducible enzyme, heme oxygenase-1 (HO-1) plays critical roles in endothelial protection (Zhao et al. 2013). In the present study, the downregulated expression of *eNOS* and *HO-1* in *IRS-2* KD cells implies that IRS-2 is a key upstream factor involved in the eNOS/HO-1 pathway in endothelial cells. VCAM-1 was identified as playing a dominant role in the initiation of atherosclerosis (Cybulsky et al. 2001), as its induction precedes monocyte adhesion and transmigration across the vascular endothelium (James et al. 2003). Our results indicates that IRS-2 might be indispensable for inhibition of *VCAM-1* expression in vascular endothelial cells. In fact, one study has demonstrated that insulin can lower the expression of VCAM-1 in endothelial cells (Rask-Madsen et al. 2010). It has been previously found that Glut-1 and Glut-2 are the major glucose transporters expressed in bovine aortic endothelial cells (Presley et al. 2010). Glut-1 and Glut-2 expression levels in *IRS-2* KD PAECs were not affected, suggesting that *IRS-2* does not affect glucose uptake in PAECs. In conclusion, the above data indicate that *IRS-2* is a valuable target gene for the generation of vascular disease models in pig.

Rodent-based models have been predominantly applied in diabetes research and have helped to understand the pathophysiologic mechanisms and to identify therapeutic targets of this disease. However, there are some problems when translating findings based on these rodent models into clinical applications. Pigs are highly similar with humans in size, anatomy, physiology, pathology, and, especially, metabolism. Unlike models that are induced by chemical treatments

or surgical methods, genetically modified pigs are advantageous for long-term and stable studies of pathophysiology and pharmacologic treatments. In this study, we successfully generated IRS-2-deficient embryos via the CRISPR/Cas9 system and SCNT. Then, we evaluated the development potential of the SCNT embryos because IRS-2 deficiency might cause developmental arrest in early embryos. Our results revealed that there is no significant difference of cleavage and blastocyst rates between IRS-2-deficient embryos and wild-type SCNT embryos.

In summary, the complete cDNA of porcine *IRS-2* was cloned for the first time. The expression and distribution patterns of porcine IRS-2 in different tissues were confirmed, and the effects of *IRS-2* knockdown on hepatocytes and endothelial function were evaluated. Further, IRS-2 knockout embryos were generated by CRISPR/Cas9 and SCNT. These results will facilitate the establishment of animal models of diabetes and vascular diseases by targeting IRS-2.

Acknowledgements

This work was supported by the "Young Talent" Project of Northeast Agricultural University (16QC31).

References

Al-Salam A, Irwin DM (**2017**) Evolution of the vertebrate insulin receptor substrate (Irs) gene family. BMC Evol Biol 17: 148.

Araki E, Lipes MA, Patti ME, Bruning JC, Haag BI, Johnson RS, Kahn CR (**1994**) Alternative pathway of insulin signalling in mice with targeted disruption of the IRS-1 gene. Nature 372: 186-190.

Choudhury AI, Heffron H, Smith MA, Al-Qassab H, Xu AW, Selman C, Simmgen M, Clements M, Claret M, Maccoll G, Bedford DC, Hisadome K, Diakonov I, Moosajee V, Bell JD, Speakman JR, Batterham RL, Barsh GS, Ashford ML, Withers DJ (**2005**) The role of insulin receptor substrate 2 in hypothalamic and beta cell function. J Clin Invest 115: 940-950.

Cybulsky MI, Iiyama K, Li H, Zhu S, Chen M, Iiyama M, Davis V, Gutierrez-Ramos JC, Connelly PW, Milstone DS (**2001**) A major role for VCAM-1, but not ICAM-1, in early atherosclerosis. J Clin Invest 107: 1255-1262.

El Mkadem SA, Lautier C, Macari F, Molinari N, Lefebvre P, Renard E, Gris JC, Cros G, Daures JP, Bringer J, White MF, Grigorescu F (**2001**) Role of allelic variants Gly972Arg of IRS-1 and Gly1057Asp of IRS-2 in moderate-to-severe insulin resistance of women with polycystic ovary syndrome. Diabetes 50: 2164-2168.

Fan N, Lai L (**2013**) Genetically modified pig models for human diseases. J Genet Genomics 40: 67-73.

Gloyn AL (**2003**) Glucokinase (GCK) mutations in hyper- and hypoglycemia: maturity-onset diabetes of the young, permanent neonatal diabetes, and hyperinsulinemia of infancy. Hum Mutat 22: 353-362.

Gribble FM (**2005**) Metabolism: a higher power for insulin. Nature 434: 965-966.

Hamamdzic D, Wilensky RL (**2013**) Porcine models of accelerated coronary atherosclerosis: role of diabetes mellitus and hypercholesterolemia. J Diabetes Res 2013: 761415.

Higashi Y, Noma K, Yoshizumi M, Kihara Y (**2009**) Endothelial function and oxidative stress in cardiovascular diseases. Circ J 73: 411-418.

Huang PL (**2009**) eNOS, metabolic syndrome and cardiovascular disease. Trends Endocrinol Metab 20: 295-302.

James WG, Bullard DC, Hickey MJ (**2003**) Critical role of the alpha 4 integrin/VCAM-1 pathway in cerebral leukocyte trafficking in lupus-prone MRL/fas(lpr) mice. J Immunol 170: 520-527.

Kerouz NJ, Horsch D, Pons S, Kahn CR (**1997**) Differential regulation of insulin receptor substrates-1 and -2 (IRS-1 and IRS-2) and phosphatidylinositol 3-kinase isoforms in liver and muscle of the obese diabetic (ob/ob) mouse. J Clin Invest 100: 3164-3172.

King GL, Park K, Li Q (**2016**) Selective Insulin Resistance and the Development of Cardiovascular Diseases in Diabetes: The 2015 Edwin Bierman Award Lecture. Diabetes 65: 1462-1471.

Koopmans SJ, Schuurman T (**2015**) Considerations on pig models for appetite, metabolic syndrome and obese type 2 diabetes: From food intake to metabolic disease. Eur J Pharmacol 759: 231-239.

Kubota N, Kubota T, Kajiwara E, Iwamura T, Kumagai H, Watanabe T, Inoue M, Takamoto I, Sasako T, Kumagai K, Kohjima M, Nakamuta M, Moroi M, Sugi K, Noda T, Terauchi Y, Ueki K, Kadowaki T (**2016**) Differential hepatic distribution of insulin receptor substrates causes selective insulin resistance in diabetes and obesity. Nature Commun 7: 12977.

Kubota T, Kubota N, Kumagai H, Yamaguchi S, Kozono H, Takahashi T, Inoue M, Itoh S, Takamoto I, Sasako T, Kumagai K, Kawai T, Hashimoto S, Kobayashi T, Sato M, Tokuyama K, Nishimura S, Tsunoda M, Ide T, Murakami K, Yamazaki T, Ezaki O, Kawamura K, Masuda H, Moroi M, Sugi K, Oike Y, Shimokawa H, Yanagihara N, Tsutsui M, Terauchi Y, Tobe K, Nagai R, Kamata K, Inoue K, Kodama T, Ueki K, Kadowaki T (**2011**) Impaired insulin signaling in endothelial cells reduces insulin-induced glucose uptake by skeletal muscle. Cell Metab 13: 294-307.

Kubota N, Tobe K, Terauchi Y, Eto K, Yamauchi T, Suzuki R, Tsubamoto Y, Komeda K, Nakano R, Miki H, Satoh S, Sekihara H, Sciacchitano S, Lesniak M, Aizawa S, Nagai R, Kimura S, Akanuma Y, Taylor SI, Kadowaki T (**2000**) Disruption of insulin receptor substrate 2 causes type 2 diabetes because of liver insulin resistance and lack of compensatory beta-cell hyperplasia. Diabetes 49: 1880-1889.

Liu ZH, Song J, Wang ZK, Tian JT, Kong QR, Zheng Z, Yin Z, Gao L, Ma HK, Sun S, Li YT, Wang HB, Prather RS (**2008**) Green fluorescent protein (GFP) transgenic pig produced by somatic cell nuclear transfer. Chin Sci Bull 53: 1035-1039.

Pardini AW, Nguyen HT, Figlewicz DP, Baskin DG, Williams DL, Kim F, Schwartz MW (**2006**) Distribution

of insulin receptor substrate-2 in brain areas involved in energy homeostasis. Brain Res 1112: 169-178.

Presley T, Vedam K, Druhan LJ, Ilangovan G (**2010**) Hyperthermia-induced Hsp90.eNOS preserves mitochondrial respiration in hyperglycemic endothelial cells by down-regulating Glut-1 and up-regulating G6PD activity. J Biol Chem 285: 38194-38203.

Rask-Madsen C, Li Q, Freund B, Feather D, Abramov R, Wu IH, Chen K, Yamamoto-Hiraoka J, Goldenbogen J, Sotiropoulos KB, Clermont A, Geraldes P, Dall'Osso C, Wagers AJ, Huang PL, Rekhter M, Scalia R, Kahn CR, King GL (**2010**) Loss of insulin signaling in vascular endothelial cells accelerates atherosclerosis in apolipoprotein E null mice. Cell Metab 11: 379-389.

Stefan N, Kovacs P, Stumvoll M, Hanson RL, Lehn-Stefan A, Permana PA, Baier LJ, Tataranni PA, Silver K, Bogardus C (**2003**) Metabolic effects of the Gly1057Asp polymorphism in IRS-2 and interactions with obesity. Diabetes 52: 1544-1550.

Taniguchi CM, Ueki K, Kahn R (**2005**) Complementary roles of IRS-1 and IRS-2 in the hepatic regulation of metabolism. J Clin Invest 115: 718-727.

Withers DJ, Burks DJ, Towery HH, Altamuro SL, Flint CL, White MF (**1999**) Irs-2 coordinates Igf-1 receptor-mediated beta-cell development and peripheral insulin signalling. Nature Genet 23: 32-40.

Withers DJ, Gutierrez JS, Towery H, Burks DJ, Ren JM, Previs S, Zhang Y, Bernal D, Pons S, Shulman GI, Bonner-Weir S, White MF (**1998**) Disruption of IRS-2 causes type 2 diabetes in mice. Nature 391: 900-904.

Wolf E, Braun-Reichhart C, Streckel E, Renner S (**2014**) Genetically engineered pig models for diabetes research. Transgenic Res 23: 27-38.

Zhang X, Lerman LO (**2016**) Investigating the Metabolic Syndrome: Contributions of Swine Models. Toxicol Pathol 44: 358-366.

Zhao Y, Zhang L, Qiao Y, Zhou X, Wu G, Wang L, Peng Y, Dong X, Huang H, Si L, Zhang X, Zhang L, Li J, Wang W, Zhou L, Gao X (**2013**) Heme oxygenase-1 prevents cardiac dysfunction in streptozotocin-diabetic mice by reducing inflammation, oxidative stress, apoptosis and enhancing autophagy. PloS One 8: e75927.